Full Characterization of Gaussian Bipartite Entangled States by a Single Homodyne Detector

V. D'Auria,[1] S. Fornaro,[1] A. Porzio,[2] S. Solimeno,[1,2] S. Olivares,[3,4] and M. G. A. Paris[4,3,5]

[1]*Dipartimento di Scienze Fisiche Università "Federico II," Napoli, Italy*
[2]*CNISM UdR Napoli Università, Napoli, Italy*
[3]*CNISM UdR Milano Università, I-20133 Milano, Italy*
[4]*Dipartimento di Fisica, Università di Milano, I-20133 Milano, Italy*
[5]*ISI Foundation, I-10133 Torino, Italy*

(Received 16 May 2008; published 13 January 2009)

We present the full experimental reconstruction of Gaussian entangled states generated by a type-II optical parametric oscillator below threshold. Our scheme provides the entire covariance matrix using a single homodyne detector and allows for the complete characterization of bipartite Gaussian states, including the evaluation of purity, entanglement, and nonclassical photon correlations, without *a priori* assumptions on the state under investigation. Our results show that single homodyne schemes are convenient and robust setups for the full characterization of optical parametric oscillator signals and represent a tool for quantum technology based on continuous variable entanglement.

DOI: 10.1103/PhysRevLett.102.020502 PACS numbers: 03.67.Mn, 03.65.Wj, 03.67.Bg, 42.65.Yj

Introduction.—In this Letter we address the complete experimental characterization of bipartite Gaussian entangled states. In our experiment continuous-wave (cw) entangled light beams are generated by a single type-II optical parametric oscillator (OPO) below threshold, and then their covariance matrix (CM) is fully reconstructed using a novel scheme [1] that involves a single homodyne detector [2]. To our knowledge this is the first *complete* characterization of OPO signals without *a priori* assumptions and paves the way to a deeper investigation of continuous variable entanglement without experimental loopholes. Light beams endowed with nonclassical correlations [3] are crucial resources for quantum technology and find applications in quantum communication [4], imaging [5], and precision measurement [6,7]. Their full characterization has a fundamental interest of its own and represents a tool for the design of quantum information processing protocols in realistic conditions. Remarkably, entangled states produced by OPOs are Gaussian states [8,9] and thus may be fully characterized by the first two statistical moments of the field modes. In turn, the CM contains the complete information about entanglement [10,11], i.e., about their performances as a resource for quantum technology. Bipartite entangled states may be generated by mixing at a beam splitter (BS) two squeezed beams obtained by a degenerate OPO below threshold [12]. The beams exiting the BS are entangled [13], and a partial reconstruction of the corresponding CM has been obtained [14]. The complete reconstruction of a CM has been obtained for different entangled states, by varying single-mode squeezing [15]. In this configuration two OPOs are used and the amount of entanglement critically depends on the symmetry between the two squeezed beams. From the experimental point of view this requires an accurate setting on the two squeezers and a strict control on the relative phase. The measured CM presents some unexpected deviations from a proper form, leaving a question open on the reliability of double homodyne schemes due to technical difficulties [14,16]. A more direct way to generate quadrature entanglement is to use a single nondegenerate OPO [17] which represents a robust and reliable source of EPR-type correlation either below [18,19] or above threshold [20–22]. Partial reconstructions of the CM in the pulsed regime has been achieved for the spectrally degenerate but spatially nondegenerate twin beams at the output of a type-I parametric amplifier [23], whereas in the cw regime cross polarized beams emitted by a self-locked type-II OPO have been examined at frequency degeneracy [16]. Although the correlation properties of OPO signals have been widely investigated, no proper CM reconstruction has been performed so far. In turn, in previous proposals and experiments nonphysical CM entries [12,14,16,23] or deviations from a proper CM [15] appeared, thus requiring *a priori* hypothesis on the measured state to understand the experimental results.

In this Letter we report the first complete measurement of the CM for the output of a single nondegenerate OPO. The two entangled beams are emitted with orthogonal polarization and degenerate frequency by a cw type-II OPO below threshold. In order to reconstruct the ten independent elements of the CM, the beams are optically combined into six auxiliary modes, whose quadratures are measured using a single homodyne detector [1]. The first two moments of the relevant quadratures are obtained by tomographic reconstruction using the whole homodyne data set. The CM is, then, fully reconstructed after assessing the Gaussian character of the signal and compared with a general model describing a realistic OPO. Entanglement is demonstrated using the partial transpose method [10], the Duan inequality [11], and the stricter EPR criterion [24], and quantified upon evaluating the logarithmic negativity and the entanglement of formation (EOF).

Reconstruction method.—Upon introducing the vector $\boldsymbol{R} = (x_1, y_1, x_2, y_2)$ of canonical operators, in terms of the mode operators a_k, $x_k = (a_k^\dagger + a_k)/\sqrt{2}$, $y_k = i(a_k^\dagger - a_k)/\sqrt{2}$, $k = 1, 2$, the CM $\boldsymbol{\sigma}$ of a bipartite state ϱ is the matrix with entries $\sigma_{hk} = \frac{1}{2}\langle\{R_k, R_h\}\rangle - \langle R_k\rangle\langle R_h\rangle$, where $\langle O\rangle = \mathrm{Tr}(\varrho O)$ and $\{f, g\} = fg + gf$. $\boldsymbol{\sigma}$ is a symmetric positive matrix, the upper and lower diagonal $2 \times$ block are denoted by A and B, respectively; C is the off-diagonal block. In the following we will use the notation $a \equiv a_1$ and $b \equiv a_2$ and also consider the four additional auxiliary modes $c = (a + b)/\sqrt{2}$, $d = (a - b)/\sqrt{2}$, $e = (ia + b)/\sqrt{2}$, and $f = (ia - b)/\sqrt{2}$ obtained by the action of polarizing beam splitters (PBS) and phase shifters on modes a and b. Positivity of the density matrix for physical states is written in terms of the uncertainty relation for the minimum symplectic eigenvalue ν_- of the CM, i.e., $\nu_- \geq 1/2$. For Gaussian states, the state purity is given by $\mu(\boldsymbol{\sigma}) = (4\sqrt{\det[\boldsymbol{\sigma}]})^{-1}$, whereas separability corresponds to $\tilde{\nu}_- > 1/2$, where $\tilde{\nu}_-$ is the minimum symplectic eigenvalue of $\boldsymbol{\Delta\sigma\Delta}$, $\boldsymbol{\Delta} = \mathrm{diag}[1, 1, 1, -1]$. A convenient measure of entanglement is thus given by the logarithmic negativity $E_{\mathcal{N}}(\boldsymbol{\sigma}) = \max(0, -\ln 2\tilde{\nu}_-)$ [25] and the EOF $E_{\mathcal{F}}(\boldsymbol{\sigma})$ can be evaluated following Ref. [26].

In our experiment, the block A of the CM is retrieved by measuring the single-mode quadratures of mode a: the variances of x_a and y_a give the diagonal elements, while the off-diagonal ones are obtained from the additional quadratures $z_a \equiv (x_a + y_a)/\sqrt{2}$ and $t_a \equiv (x_a - y_a)/\sqrt{2}$ as $\sigma_{12} = \sigma_{21} = \frac{1}{2}(\langle z_a^2\rangle - \langle t_a^2\rangle) - \langle x_a\rangle\langle y_a\rangle$ [1]. The block B is reconstructed in the same way from the quadratures of b, whereas the elements of the block C are obtained from the quadratures of the auxiliary modes c, d, e , and f as follows: $\sigma_{13} = \frac{1}{2}(\langle x_c^2\rangle - \langle x_d^2\rangle) - \langle x_a\rangle\langle x_b\rangle$, $\sigma_{14} = \frac{1}{2} \times (\langle y_e^2\rangle - \langle y_f^2\rangle) - \langle x_a\rangle\langle y_b\rangle$, $\sigma_{23} = \frac{1}{2}(\langle x_f^2\rangle - \langle x_e^2\rangle) - \langle y_a\rangle\langle x_b\rangle$, $\sigma_{24} = \frac{1}{2}(\langle y_c^2\rangle - \langle y_d^2\rangle) - \langle y_a\rangle\langle y_b\rangle$. Notice that the measurement of the f quadratures is not mandatory, since $\langle x_f^2\rangle = \langle x_b^2\rangle + \langle y_a\rangle^2 - \langle x_e^2\rangle$ and $\langle y_f^2\rangle = \langle x_a^2\rangle + \langle y_b^2\rangle - \langle y_e^2\rangle$. Analogous expressions hold for $\langle x_e^2\rangle$ and $\langle y_e^2\rangle$.

In the ideal case the OPO output is in a twin-beam state $\mathbf{S}(\zeta)|0\rangle$, $\mathbf{S}(\zeta) = \exp\{\zeta a^\dagger b^\dagger - \bar{\zeta} ab\}$ being the entangling two-mode squeezing operator: the corresponding CM has diagonal blocks A, B, C with the two diagonal elements of each block equal in absolute value. In realistic OPOs, cavity and crystal losses lead to a mixed state, i.e., to an effective thermal contribution. In addition, spurious nonlinear processes, not perfectly suppressed by the phase matching, may combine to the down conversion, contributing with local squeezings. Finally, due to small misalignments of the nonlinear crystal, a residual component of the field polarized along a may project onto the orthogonal polarization (say along b), thus leading to a mixing among the modes [27]. Overall, the state at the output is expected to be a zero amplitude Gaussian entangled state, whose general form may be written as $\varrho_g = \mathbf{U}(\beta)\mathbf{S}(\zeta)\mathbf{LS}(\xi_1, \xi_2)\mathbf{TLS}^\dagger(\xi_1, \xi_2)\mathbf{S}^\dagger(\zeta)\mathbf{U}^\dagger(\beta)$, where $\mathbf{T} = \tau_1 \otimes \tau_2$, with $\tau_k = (1 + \bar{n}_k)^{-1}[\bar{n}_k/(1 + \bar{n}_k)]^{a^\dagger a}$ denotes a two-mode thermal state with $\bar{n}_k$ average photons per mode, $\mathbf{LS}(\xi_1, \xi_2) = S(\xi_1) \otimes S(\xi_2)$, $S(\xi_k) = \exp\{\frac{1}{2} \times (\xi_k a^{\dagger 2} - \bar{\xi}_k a^2)\}$ denotes local squeezing, and $\mathbf{U}(\beta) = \exp\{\beta a^\dagger b - \bar{\beta} ab^\dagger\}$ a mixing operator, ζ, ξ_k, and β being complex numbers. For our configuration, besides a thermal contribution due to internal and coupling losses, we expect a relevant entangling contribution with a small residual local squeezing and a possible mixing among the modes. The CM matrix corresponding to ϱ_g has diagonal blocks A, B, and C with possible asymmetries among the diagonal elements.

Experimental setup.—The experimental setup, shown in Fig. 1, relies on a cw internally frequency doubled Nd:YAG laser pumping (at 532 nm) a nondegenerate OPO based on a periodically poled α-cut potassium tytanil phosphate (PPKTP) crystal (Raicol Crystals Ltd. on custom design) [28]. The use of the α-cut PPKTP allows implementing a type-II phase matching with cross polarized signal (a) and idler (b) waves, frequency degenerate at 1064 nm for a crystal temperature of $\approx 53\,^\circ$C. The OPO cavity is locked to the pump beam by Pound-Drever technique [29] and adjusted to work in triple resonance by finely tuning its geometrical properties [27]. The cavity output coupling at 1064 nm is ≈ 0.73, corresponding to an experimental line width of 16 MHz at 1064 nm. The measured oscillation threshold is $P_{\mathrm{th}} \approx 50$ mW; during the acquisition the system has been operated below threshold at 60% of the threshold power. In order to select mode a and b or their combinations c and d, the OPO beams are sent to a half-wave plate and a PBS. Modes e and f are obtained by inserting an additional quarter-wave plate [1]. The PBS output goes to a homodyne detector, described in detail in [7,30], exploiting the laser output at 1064 nm as local oscillator (LO). The overall homodyne detection efficiency is $\eta = 0.88 \pm 0.02$. The LO reflects on a piezomounted mirror (PZT), which allows varying its phase θ. In order to avoid the laser low frequency noise, data sampling is moved away from the optical carrier frequency by $\Omega = 3$ MHz [30]. The resulting current is low-pass

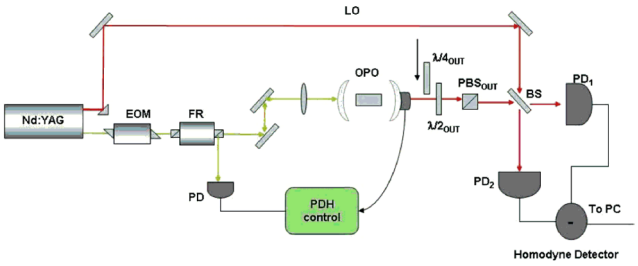

FIG. 1 (color online). Experimental setup: A type-II PPKTP-OPO is pumped by the second harmonic of a Nd:YAG laser. At the OPO output, a half- and a quarter-wave plate and a PBS select the mode for homodyning.

filtered ($B = 300$ kHz) and sampled by an acquisition board (gage 14 100, 1 M points per run, 14 bits resolution). The total electronic noise power has been measured to be 16 dBm below the shot-noise level, corresponding to a signal to noise ratio of about 40.

Reconstruction and experimental results.—Acquisition is triggered by a linear ramp applied to the PZT and adjusted to obtain a 2π variation in 200 ms. Upon spanning the LO phase θ, the quadratures $x(\theta) = x\cos\theta + y\sin\theta$ are measured. All the expectation values needed to reconstruct $\boldsymbol{\sigma}$ are obtained by quantum tomography [31], which allows us to compensate nonunit quantum efficiency and to reconstruct any expectation value, including those of specific quadratures and their variances, by averaging special pattern functions over the whole data set. As a preliminary check of the procedure, we verified that the CM of the vacuum state is consistent with $\boldsymbol{\sigma}_0 = \frac{1}{2}\mathbb{I}$ within the experimental errors. At first we checked (i) the Gaussian character of the signals by the kurtosis of homodyne distribution at fixed phase [30] and (ii) the absence of the signals' amplitude since the mean values of all the involved quadratures are negligible. Then, we measured the quadratures of the six modes a–f. We found the modes a and b excited in a thermal state, thus confirming the absence of relevant local squeezing. Their combinations c, d, e, and f are squeezed thermal states with squeezing appearing on y_c, x_d, t_e, and z_f, respectively. In Fig. 2 we show the experimental homodyne traces for modes c and d as well as the corresponding Wigner functions, obtained by reconstructing the single-mode CM. As it is apparent from the plots, both modes are squeezed with quadrature noise reduction, corrected for nonunit efficiency, of about 2.5 dB. An analogue behavior has been observed for modes e and f. The CM of Fig. 2 indeed reproduces that of an entangled thermal state with small corrections due to local squeezing and mixing. The relevant parameters to characterize the corresponding density matrix ϱ_g are the mean number of thermal photons $\bar{n}_1 \simeq 0.67$, $\bar{n}_2 \simeq 0.18$ and entangling photons $\bar{n}_s = 2\sinh^2|\zeta| \simeq 0.87$ [32]. The errors on the CM elements for the blocks A and B are of the order $\delta\sigma_{jk} \simeq 0.004$ and have been obtained by propagating the tomographic errors. In this case phase fluctuations are irrelevant, since the two modes are both excited in a thermal state. On the other hand, in evaluating the errors on the elements of the block C the phase-dependent noise properties of the involved modes have to be taken into account, and the tomographic error has to be compared with the error due to the finite accuracy in setting the LO phase θ. The elements σ_{13} and σ_{24} are obtained as combinations of squeezed/antisqueezed variances, which are quite insensitive to fluctuations of θ. As a consequence the errors on these elements are given by the overall tomographic error $\delta\sigma_{jk} \simeq 0.004$. On the other hand, the elements σ_{14} and σ_{23} depend on the determination of $x^2_{e,f}$ and $y^2_{e,f}$, which are sensible to phase fluctuations. In order to take into account

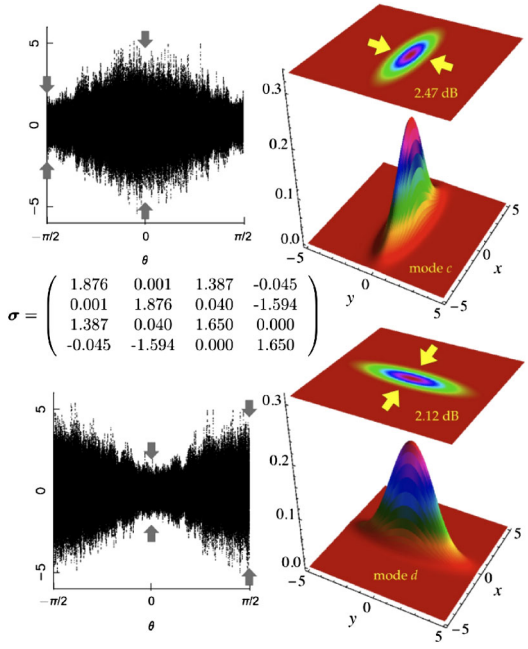

FIG. 2 (color online). Left: Experimental homodyne traces and reconstructed CM; right: reconstructed Wigner functions. Top plots are for mode c and bottom ones for d. Arrows on the homodyne plots show the maximum and minimum variances. θ is the relative phase between the signal and the LO.

this effect we evaluate errors as the fluctuations in the tomographically reconstructed quadratures induced by a $\delta\theta \simeq 20$ mrad variation in the LO phase, corresponding to the experimental phase stability of the homodyne detection. The resulting errors are about $\delta\sigma_{14} = \delta\sigma_{23} \simeq 0.03$ for both CM elements. The off-diagonal elements of the three matrices A, B, and C are thus zero within their statistical errors. The experimental procedure may be somehow simplified exploiting the relationships among modes, and expressing mode e or f in terms of the others: only five modes are then needed. Upon rewriting the off-diagonal terms of C in terms of the five modes we arrive at $\sigma_{14} = 0.02 \pm 0.03$ and $\sigma_{23} = 0.04 \pm 0.03$ when eliminating the mode f and $\sigma_{14} = 0.06 \pm 0.03$ and $\sigma_{23} = 0.06 \pm 0.03$ when eliminating the mode e. Both procedures provide results in agreement with those obtained by using the complete set of homodyne data for the six modes.

Since the minimum symplectic eigenvalue of $\boldsymbol{\sigma}$ is $\nu_- = 0.68 \pm 0.02 \geq 0.5$, the CM corresponds to a physical state. State purity is $\mu(\boldsymbol{\sigma}) = 0.31 \pm 0.01$. The minimum symplectic eigenvalue for the partial transpose is $\tilde{\nu}_- = 0.24 \pm 0.02$, which corresponds to a logarithmic negativity $E_{\mathcal{N}}(\boldsymbol{\sigma}) = 0.73 \pm 0.02$; i.e., the state is entangled, with EOF $E_{\mathcal{F}}(\boldsymbol{\sigma}) = 1.46 \pm 0.02$. In turn, it satisfies the Duan inequality with the results $0.29 \pm 0.01 < 1/2$ and the EPR criterion with $0.21 \pm 0.01 < 1/4$. Entangled Gaussian states as ϱ_g may be endowed with nonclassical photon number correlations, i.e., squeezing in the difference photon number. This may be checked upon

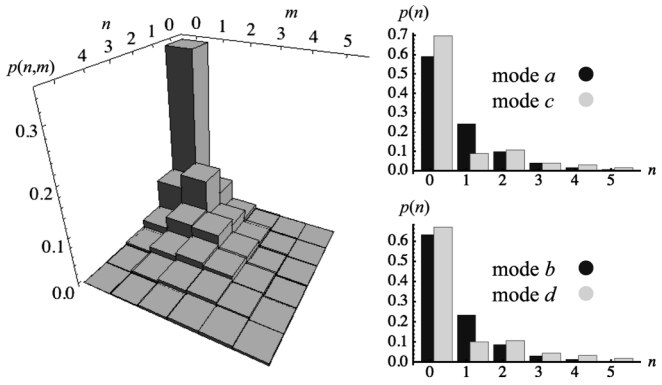

FIG. 3. Left: Joint photon number distribution $p(n, m)$ for the entangled state of modes a and b at the output of the OPO. Right: Single-mode photon distributions $p(n)$ for modes a and c (top right) and b and d (bottom right). The single-mode distributions of modes a and b are thermal and correspond to the marginals of $p(n, m)$. The distributions for modes c and d are those of squeezed thermal states.

evaluating the noise reduction factor $\mathcal{R} = \mathrm{Var}(D_{ab})/(\bar{N}_a + \bar{N}_b)$, where $\mathrm{Var}(D_{ab})$ denotes the variance of the difference photocurrent $D_{ab} = N_a - N_b$, $N = a^\dagger a$ being the number operator, and $\bar{N}_k = \langle N_k \rangle$ the average photon number. A value $\mathcal{R} < 1$ is a marker of nonclassical correlations between the two modes. We obtained $\mathcal{R} = 0.50 \pm 0.02$, in agreement with the theoretical description [33] for the values of thermal and entangling photons reported above. Starting from the CM one can reconstruct the full joint photon distribution $p(n, m)$ of the modes a and b: the result is shown in Fig. 3 where the correlations between the two modes are clearly seen. We have also evaluated the single-mode photon distributions (either from data or from the single-mode CM) for modes a–d. Results are reported in Fig. 3: distributions of a and b are thermal, whereas the statistics of modes c and d correctly reproduces the even-odd oscillations expected for squeezed thermal states.

Conclusion.—We have presented the complete reconstruction of the CM for the output of a cw type-II nondegenerate OPO, below threshold and frequency degenerate. The quantities of interest have been obtained tomographically, processing the whole data set and thus reducing statistical fluctuations. Upon exploiting a general model allowing local squeezing and polarization cross talking inside the crystal, we have very precisely described the experimental CM with the theory underlying parametric down-conversion. The reconstructed state is a Gaussian entangled state close to a two-mode squeezed thermal state, the corresponding entanglement and nonclassical photon number correlations have been demonstrated. We conclude that single homodyne schemes are convenient and robust setups for the full characterization of OPO signals and, in turn, represent a relevant tool for quantum technology based on CV entanglement, e.g., the full characterization of CV Gaussian channels by input-output signals' characterization. Finally, making use of a single OPO and a single homodyne detector, our setup also represents a compact and robust tool for entanglement generation and characterization.

This work has been partially supported by CNR-CNISM. M. G. A. P. thanks M. Bondani and A. Allevi for discussions.

[1] V. D'Auria *et al.*, J. Opt. B **7**, S750 (2005); A. Porzio *et al.*, Int. J. Quantum. Inform. **5**, 63 (2007).
[2] M. G. Raymer and A. Funk, Phys. Rev. A **61**, 015801 (1999); D. F. McAlister and M. G. Raymer, J. Mod. Opt. **44**, 2359 (1997).
[3] J. Eisert *et al.*, Int. J. Quantum. Inform. **1**, 479 (2003); A. Ferraro *et al.*, *Gaussian States in Quantum Information* (Bibliopolis, Napoli, 2005); G. Adesso *et al.*, J. Phys. A **40**, 7821 (2007); S. L. Braunstein *et al.*, Rev. Mod. Phys. **77**, 513 (2005).
[4] P. van Loock, Fortschr. Phys. **50**, 1177 (2002).
[5] L. A. Lugiato *et al.*, J. Opt. B **4**, S176 (2002).
[6] G. M. D'Ariano *et al.*, Phys. Rev. Lett. **87**, 270404 (2001).
[7] V. D'Auria *et al.*, J. Phys. B **39**, 1187 (2006).
[8] R. Simon *et al.*, Phys. Rev. A **36**, 3868 (1987); Phys. Rev. A **49**, 1567 (1994).
[9] P. Marian *et al.*, Phys. Rev. A **47**, 4474 (1993); **47**, 4487 (1993); **68**, 062309 (2003).
[10] R. Simon, Phys. Rev. Lett. **84**, 2726 (2000).
[11] L.-M. Duan *et al.*, Phys. Rev. Lett. **84**, 2722 (2000).
[12] W. P. Bowen *et al.*, Phys. Rev. Lett. **90**, 043601 (2003).
[13] M. G. A. Paris, Phys. Lett. A **225**, 28 (1997); X. B. Wang, Phys. Rev. A **66**, 024303 (2002).
[14] W. P. Bowen *et al.*, Phys. Rev. A **69**, 012304 (2004).
[15] J. Di Guglielmo *et al.*, Phys. Rev. A **76**, 012323 (2007).
[16] J. Laurat *et al.*, J. Opt. B **7**, S577 (2005).
[17] P. D. Drummond *et al.*, Phys. Rev. A **41**, 3930 (1990).
[18] Y. Zhang *et al.*, Phys. Lett. A **259**, 171 (1999).
[19] Z. Y. Ou *et al.*, Phys. Rev. Lett. **68**, 3663 (1992).
[20] J. Jing *et al.*, Phys. Rev. A **74**, 041804 (2006).
[21] A. S. Villar *et al.*, J. Opt. Soc. Am. B **24**, 249 (2007).
[22] G. Keller *et al.*, Opt. Express **16**, 9351 (2008).
[23] J. Wenger *et al.*, Eur. Phys. J. D **32**, 391 (2005).
[24] N. Treps *et al.*, Laser Phys. **15**, 187 (2005).
[25] G. Vidal *et al.*, Phys. Rev. A **65**, 032314 (2002).
[26] P. Marian and T. A. Marian, Phys. Rev. Lett. **101**, 220403 (2008).
[27] V. D'Auria *et al.*, Appl. Phys. B **91**, 309 (2008).
[28] M. M. Fejer *et al.*, IEEE J. Quantum Electron. **28**, 2631 (1992).
[29] R. W. P. Drever *et al.*, Appl. Phys. B **31**, 97 (1983).
[30] V. D'Auria *et al.*, Opt. Express **13**, 948 (2005).
[31] G. M. D'Ariano *et al.*, Adv. Imaging Electron Phys. **128**, 205 (2003).
[32] The other parameters are given by $\xi_1 \simeq 0.07e^{i0.12\pi}$, $\xi_2 \simeq 0.12e^{-i0.12\pi}$, $\beta \simeq 0.13\pi e^{-i0.17\pi}$.
[33] I. P. Degiovanni *et al.*, Phys. Rev. A **76**, 062309 (2007).